AIMS Mathematics, 9(2): 3505–3520.
DOI: 10.3934/math.2024172
Received: 05 November 2023
Revised: 30 December 2023
Accepted: 02 January 2024
Published: 08 January 2024

http://www.aimspress.com/journal/Math

Research article

Research on nonlinear infectious disease models influenced by media factors and optimal control

Danni Wang, Hongli Yang* and Liangui Yang

School of Mathematical Sciences, Inner Mongolia University, Hohhot 010021, China

* **Correspondence:** Email: imuyhl@imu.edu.cn.

Abstract: In this article, a mathematical model was developed to describe disease control by media factors. The Lambert W function was used to convert the system definition by implicit functions into explicit functions. We analyzed the dynamics of the defined piecewise smooth system and verified the correctness of the theoretical analysis through numerical simulation. Research revealed that media factors can delay the peak of an epidemic and reduce the scale of the epidemic. It is worth noting that adopting different control measures has a certain impact on the scale of the epidemic; the analysis results indicate that implementing dual-control is the most effective way to limit the spread of diseases and this strategy may provide clues for disease control.

Keywords: SIR epidemic model; optimal control; dynamic; media factors; Lambert W function
Mathematics Subject Classification: 65P40, 92D30, 93E20

1. Introduction

The 2019 Coronavirus disease (COVID-19) originated from a new type of severe acute respiratory syndrome coronavirus [1]. According to existing cases data, some patients may experience respiratory and digestive symptoms such as nasal congestion, runny nose, and diarrhea [2, 3]. In severe cases, they may rapidly progress to acute respiratory distress syndrome, septic shock, difficulty to correct metabolic acidosis, coagulation disorders, and multiple organ failure [3]. It should be noted that elderly people and those with chronic underlying diseases have a poorer preventive capacity and the symptoms of youngster cases are relatively mild [4, 5]. During the sudden outbreak of an epidemic, for avoiding cross infection of patients with multiple strains [6], it is important to practice self-protection, wash hands frequently, maintain good hygiene habits, raise health awareness, correctly wear disposable masks, avoid contact with infected individuals, and avoid going to dangerous crowded and enclosed places [7].

Media factors play a crucial role in the outbreak of an epidemic [8, 9]. They can detect and report

an epidemic early, provide a warning, and use public opinion to take effective measures to eliminate potential crises before they escalate [10, 11]. By disseminating information about the epidemic, the media can help the public understand its severity and better control its development [12]. During the initial phases of the Severe acute respiratory syndrome coronavirus (SARS) outbreak in 2003, various speculations were circulating amongst the general public, causing widespread social unrest due to insufficient dissemination of information regarding SARS prevention and treatment [13, 14]. During COVID-19, the media disseminated information to assist medical personnel and warn the public to prioritize personal protection, contributing significantly to guiding public perception. This statement highlights the need to explore how media coverage impacts the transmission and management of infectious diseases.

Mathematical models have the ability to predict disease development trends through dynamic analysis [15–19]. Currently, numerous studies have established mathematical models to simulate the dynamics of COVID-19 [20–22]. Jia and his colleagues proposed a dynamic model of COVID-19 based on official data to analyze the impact of non-pharmaceutical interventions on transmission dynamics during the COVID-19 pandemic [20]. Huang et al. established a COVID-19 mathematical model to analyze how spontaneous social distance and public social distance can increase the outbreak threshold of asymptomatic infections [21]. Maji et al. theoretically and numerically revealed that social distance has a significant impact on reducing the spread of COVID-19 [22]. Mathematical models are powerful in simulating the impact of various factors on diseases and offer optimal control strategies for disease control.

The remaining of this article is as follows: In Section 2, a mathematical model is proposed, which includes media related factors, and the properties of the Lambert W function are used to convert the system into an explicitly defined system through an implicit function. This system is a piecewise smooth system that can analyze the dynamic of the system. In Section 3, we study the dynamics of the piecewise smooth system, as well as the existence and local stability of endemic equilibrium points. In Section 4, the impact of various control methods on infectious diseases is modeled using optimal control theory. In Section 5, the numerical simulation results verify the theoretical analysis results and uncover that media factors can affect the scale of epidemic outbreaks. The results show that implementing the dual-control strategy is the most effective way to limit the spread of diseases, which may provide clues for disease control.

2. Model description

The dynamics in susceptible population $S(t)$, infected population $I(t)$, and convalescent population $R(t)$ are considered. The exponential factor of $I(t)$ is used to express the media influence on the infectious diseases, similar to reference [12], the function is defined as $f(I) = be^{-}N(I, \frac{dI}{dt})$, and $N(I, \frac{dI}{dt})$ is shown as follows:

$$N(I, \frac{dI}{dt}) = m_1 I(t) + m_2 \frac{dI(t)}{dt}$$

where $m_1, m_2 \in \mathbf{R}$, it is assumed that m_1 represents government or official media news coverage, and m_2 represents media news reports related to medical prevention. If $m_1, m_2 < 0$ represents false news factors misleading the public, the function $f(I)$ is monotonically increasing. If $m_1, m_2 \geq 0$, which means that fake news will be perceived by the public and corrected by the government or official institutions while

real news dominates public opinion, then the function $f(I)$ will monotonically decrease. Based on the properties of function $f(I)$, we focus on the control effect of real news on infectious diseases and we set m_1 and m_2 as nonnegative parameters, which are used to represent the impact of real news factors on media coverage cases and change rates. The function $N(t) = N(I, \frac{dI}{dt})$ is transformed into the following form:

$$N(I, \frac{dI}{dt}) = \max\left\{0, m_1 I(t) + m_2 \frac{dI(t)}{dt}\right\}.$$

For the $R(t)$ population after recovery, they will no longer impose risk on susceptible individuals. In most studies, the model is established by assuming that the total population is constant or satisfies exponential growth [23, 24]. A new epidemic dynamic model is obtained as follows:

$$\begin{cases} \dfrac{\mathrm{d}S}{\mathrm{d}t} = aS(1 - \dfrac{S}{k}) - e^{-N(I,\frac{dI}{dt})}bIS, \\ \dfrac{\mathrm{d}I}{\mathrm{d}t} = e^{-N(I,\frac{dI}{dt})}bIS - \alpha I - \beta I - \gamma I, \\ \dfrac{\mathrm{d}R}{\mathrm{d}t} = \gamma I - \mu R. \end{cases} \tag{2.1}$$

In model (2.1), all parameters are positive based on theoretical facts and the meaning of each parameter is as follows: a is the inherent growth rate of population and k is the population carrying capacity of a given region. We hypothesize b as the basic propagation coefficient and $f(I) = be^{-N(I,\frac{dI}{dt})}$ is the term of contact and transmission, which measures the spread of the virus from susceptible individuals to infected individuals. α is the mortality rate associate with the disease, β is the natural death rate, γ is the rate of recovery from infection, and μ is the death caused by the sequela of disease recovery. To simplify, let $n = \alpha + \beta + \gamma$ and $N_1(t) = m_1 I(t) + m_2 \frac{dI}{dt}$ when $N_1(t) > 0$, then $N_1(t) = N(t)$. Following from the second equation in (2.1), we can get

$$m_2(\frac{dI}{dt} + nI)e^{m_2(nI+\frac{dI}{dt})} = m_2 bS\, Ie^{-m_1 I + m_2 nI}. \tag{2.2}$$

It can be observed that the form of Eq (2.2) is quite complex, so we introduce the definition and properties of the Lambert W function, which are

Definition 1 ([25]). *The Lambert W function is the inverse of the function $f(z) = ze^z$ and satisfies the following conditions*

$$Lambert\ W(z) \cdot exp(Lambert\ W(z)) = z.$$

By definition, we have

$$Lambert\ \dot{W}(z) = \frac{Lambert\ W(z)}{z + (Lambert\ W(z))}.$$

Using the definition of Lambert W function, we can obtain

$$\frac{\mathrm{d}I}{\mathrm{d}t} = \frac{1}{m_2}\mathrm{W}[m_2 bS\, Ie^{-m_1 I + m_2 nI}] - nI. \tag{2.3}$$

Therefore, $N(t)$ reads

$$\begin{aligned} N(t) =& N_1(t) = m_1 I + m_2 \frac{dI}{dt} \\ =& \mathrm{W}[m_2 bS\, I e^{-m_1 I + m_2 nI}] - (-m_1 I + m_2 nI). \end{aligned} \tag{2.4}$$

We study that $N_1(t)$ is greater than zero; for this, we consider $N_1(t)$ equal to 0, then

$$\mathrm{W}[m_2 bS\, I e^{-m_1 I + m_2 nI}] - (-m_1 I + m_2 nI) = 0. \tag{2.5}$$

We use the properties of the Lambert W function, then

$$(-m_1 I + m_2 nI) e^{-m_1 I + m_2 nI} = m_2 bS\, I e^{-m_1 I + m_2 nI} \tag{2.6}$$

and we obtain

$$S = \frac{m_2 n - m_1}{b m_2} = S_q. \tag{2.7}$$

Because $N_1(t) > 0$ is strictly monotone for S, it yields that $N_1(t) > 0$ is equivalent to $S > S_q$. In order to study the properties of the epidemic model, we remove the equation of the individual $R(t)$, and system (2.1) is transformed into system (2.8)

$$\begin{cases} \dfrac{\mathrm{d}S}{\mathrm{d}t} = aS(1 - \dfrac{S}{k}) - e^{-\theta N_1(t)} bIS, \\ \dfrac{\mathrm{d}I}{\mathrm{d}t} = e^{-\theta N_1(t)} bIS - \alpha I - \beta I - \gamma I \end{cases} \tag{2.8}$$

with

$$\theta = \begin{cases} 0, S - S_q \le 0, \\ 1, S - S_q \ge 0. \end{cases} \tag{2.9}$$

Equations (2.8) and (2.9) indicate that the system has a susceptibility threshold, and there is no influence of media factors below the threshold. Above the threshold, the media has a certain role in reducing the spread of disease, so the media has a certain impact on the disease. The susceptibility threshold is analyzed in the following content.

We set $P(Z) = S - S_q$ with $X = (S, I)^T$, then

$$\begin{aligned} P_{A_1}(Z) &= (aS(1 - \frac{S}{k}) - bIS, bIS - \alpha I - \beta I - \gamma I)^T, \\ P_{A_2}(Z) &= (aS(1 - \frac{S}{k}) - e^{-\theta M_1} bIS, e^{-\theta M_1} bIS - \alpha I - \beta I - \gamma I)^T. \end{aligned}$$

The Eqs (2.8) and (2.9) become a non-smooth system

$$\dot{X}(t) = \begin{cases} P_{A_1}(X), X \in A_1, \\ P_{A_2}(X), X \in A_2 \end{cases} \tag{2.10}$$

with

$$A_1 = \{X \in R_+^2 : J(X) \leq 0\},$$

$$A_2 = \{X \in R_+^2 : J(X) > 0\}$$

and the system (2.1) invariant set is $R_+^2 = \{X = (S, I), S \geq 0, I \geq 0\}$. If $-m_1 + m_2 n > 0$ holds, we have $S_q > 0$; if $S_q < 0$, the set A_1 becomes an empty set, then the non-smooth system (2.10) becomes smooth system $\dot{X}(t) = P_{A_2}(X)$.

The switching line defined by Ξ is

$$\Xi = \{X \in R^2 : J(X) = 0\}.$$

Therefore, the system (2.10) is located in region A_1 or A_2 recorded as S_{A1} or S_{A2}, respectively. We use the properties of the Lambert W function to transform the implicitly defined function system (2.1) into a piecewise smooth (PWS) system [26]. The equilibrium point of PWS (2.10) as follows:

Theorem 1 ([12]). *If $P_{A_1}(X^*) = 0, J(X^*) \leq 0$ or $P_{A_2}(Z^*) = 0, J(X^*) > 0$, the point X^* is the regular equilibrium of system* (2.10)*; if $P_{A_1}(X^*) = 0, J(X^*) > 0$ or $P_{A_2}(X^*) = 0, J(X^*) \leq 0$, X^* is the virtual equilibrium point.*

3. The dynamics of PWS system

In this part, we analyze the different areas S_{A1} and S_{A2} to study the dynamics of the system (2.10).

The dynamics of S_{A1}. The system dynamics of S_{A1} have a disease-free equilibrium point E_0^*, which is $(k, 0)$, then

$$k - S_q = \frac{m_2(R_0 - 1) + m_1}{bm_2}.$$

When $R_0 = kb/n > -\frac{m_1}{m_2} + 1$, the point E_0^* is in the area S_{A_2}, and when $R_0 < -\frac{m_1}{m_2} + 1$, the equilibrium point E_0^* is locally stable in S_{A1}. The interior equilibrium point $\tilde{E}_1 = (\tilde{S}_1, \tilde{I}_1)$ of S_{A1} exists only if $R_0 > 1$, and

$$\tilde{S}_1 = \frac{n}{b}, \tilde{I}_1 = \frac{a}{b}(kb/n - 1) = \frac{a}{b}(R_0 - 1).$$

Note that $\tilde{S}_1 > S_q$ holds, which means that equilibrium $\tilde{E}_1$ is located in region S_{A_2}, so it is a virtual equilibrium.

The dynamics of S_{A2}. For the smooth system S_{A2}, the equation is as follows

$$\begin{cases} \dfrac{\mathrm{d}S}{\mathrm{d}t} = aS(1 - \dfrac{S}{k}) - e^{-N_1(t)}bIS, \\ \dfrac{\mathrm{d}I}{\mathrm{d}t} = e^{-N_1(t)}bIS - \alpha I - \beta I - \gamma I, \end{cases} \quad S > S_c. \tag{3.1}$$

Because $N_1(t)$ contains the Lambert W function, it is difficult to study its dynamics through theoretical analysis. The disease-free equilibrium of system (3.1) is $E_0^* = (k, 0)$, which is consistent with the corresponding of system S_{A1}.

Existence of endemic equilibrium.

Lemma 1. *The interior equilibrium point $\tilde{E}_2 = (S^*, I^*)$ is located in the area of A_2 and it is a regular equilibrium, where*

$$S^* = \frac{n}{b}e^{m_1 I^*}, I^* = \frac{a}{b}e^{m_1 I^*}(1 - \frac{n}{kb}e^{m_1 I^*}).$$

Proof. In the function $N_1(t)$, we define

$$G_1(S, I) \triangleq m_2 bSIe^{-m_1 I + m_2 nI}, G_2(I) \triangleq -m_1 I + m_2 nI$$

then

$$N_1(t) = \mathrm{W}(G_1(S, I)) - G_2(I)$$

and by using the properties of the Lambert W function, we can get

$$\begin{aligned} exp(-N_1(t)) =& exp(-\mathrm{W}(G_1(S, I)) + G_2(I)) \\ =& \frac{\mathrm{W}(G_1(S, I))}{G_1(S, I)} exp(G_2(I)) = \frac{\mathrm{W}(G_1(S, I))}{m_2 bSI}. \end{aligned} \tag{3.2}$$

Substituting Eq (3.2) into model (3.1), we have

$$\begin{cases} \frac{\mathrm{d}S}{\mathrm{d}t} = aS(1 - \frac{S}{k}) - \frac{\mathrm{W}(G_1(S, I))}{m_2}, \\ \frac{\mathrm{d}I}{\mathrm{d}t} = \frac{\mathrm{W}(G_1(S, I))}{m_2} - nI, \end{cases} \quad S > S_c. \tag{3.3}$$

If the second of the above formulas is equal to zero, then there is $\mathrm{W}(G_1(S, I)) = m_2 nI$. Utilizing the properties of the Lambert W function, we can obtain

$$S^* = \frac{n}{b}e^{m_1 I^*}. \tag{3.4}$$

Substituting (3.4) into the first formula in (3.3) and combining with $\mathrm{W}(G_1(S, I)) = m_2 nI$, we get

$$\frac{an}{b}e^{m_1 I^*}(1 - \frac{n}{kb}e^{m_1 I^*}) = nI^*, \tag{3.5}$$

$$I^* = \frac{a}{b}e^{m_1 I^*}(1 - \frac{n}{kb}e^{m_1 I^*}). \tag{3.6}$$

We consider $I^* > 0$, and the parameters are all positive, that is,

$$(1 - \frac{n}{kb}e^{m_1 I^*}) > 0 \tag{3.7}$$

which is equivalent to

$$R_0 = \frac{kb}{n} > e^{m_1 I^*} > 1. \tag{3.8}$$

If $R_0 > 1$, the interior equilibria $\tilde{E}_2 = (S^*, I^*)$ satisfies condition $S^* > S_q$, which means that $\tilde{E}_2$ is located in the area of A_2 and it is a regular equilibrium. □

Local stability of the endemic equilibrium $\tilde{E}_2$.

Lemma 2. *If the parameters satisfy the following relationship*

$$-\frac{T_2}{m_2}+n+\frac{T_1}{m_2}-a+\frac{2aS^*}{k}>0,$$

$$\frac{nT_1}{m_2}+\frac{aT_2}{m_2}-\frac{2aT_2S^*}{m_2k}-a+\frac{2aS^*}{k}>0,$$

$$(-\frac{T_2}{m_2}+n+\frac{T_1}{m_2}-a+\frac{2aS^*}{k})^2-4(\frac{nT_1}{m_2}+\frac{aT_2}{m_2}-\frac{2aT_2S^*}{m_2k}-a+\frac{2aS^*}{k})>0$$

then the system (3.3) *has the point $\tilde{E}_2$ as locally asymptotically stable.*

Proof. We use the Jacobian matrix to analyze the stability of equilibrium point $\tilde{E}_2$ and set $c=-m_1+m_2n$ and

$$\begin{aligned} D_1(S,I) =& aS(1-\frac{S}{k})-\frac{\mathrm{W}(G_1(S,I))}{m_2},\\ D_2(S,I) =& \frac{\mathrm{W}(G_1(S,I))}{m_2}-nI. \end{aligned} \tag{3.9}$$

The Jacobian matrix is as follows

$$J=\begin{pmatrix} \frac{\partial D_1}{\partial S} & \frac{\partial D_1}{\partial I}\\ \frac{\partial D_2}{\partial S} & \frac{\partial D_2}{\partial I}\end{pmatrix}=\begin{pmatrix} -\frac{1}{m_2}T_1+a-\frac{2aS}{k} & -\frac{1}{m_2}T_2\\ -\frac{1}{m_2}T_1 & \frac{1}{m_2}T_2-n\end{pmatrix} \tag{3.10}$$

where T_1 and T_2 are defined as

$$T_1=\frac{\partial \mathrm{W}(G_1(S,I))}{\partial S}=\frac{\mathrm{W}(G_1(S,I))}{G_1(S,I)(1+\mathrm{W}(G_1(S,I)))}\frac{\partial G_1}{\partial S},$$

$$T_2=\frac{\partial \mathrm{W}(G_1(S,I))}{\partial I}=\frac{\mathrm{W}(G_1(S,I))}{G_1(S,I)(1+\mathrm{W}(G_1(S,I)))}\frac{\partial G_1}{\partial I}$$

with

$$\frac{\partial G_1}{\partial S}=m_2bIe^{cI},\quad \frac{\partial G_1}{\partial I}=m_2bIe^{cI}(1+cI).$$

In order to simplify the calculation at the equilibrium point $\tilde{E}_2$, we can get

$$\begin{aligned} T_1 =& \frac{m_2nI^*}{G_1(S^*,I^*)(1+m_2nI^*)}m_2bI^*e^{cI^*}=\frac{m_2nI^*}{S^*(1+m_2nI^*)},\\ T_2 =& \frac{m_2nI^*}{G_1(S^*,I^*)(1+m_2nI^*)}m_2bS^*e^{cI^*}(1+cI^*)=\frac{m_2n(1+cI^*)}{S^*(1+m_2nI^*)}. \end{aligned} \tag{3.11}$$

Thus, the characteristic equation at point $\tilde{E}_2$ is

$$\begin{aligned} \lambda^2+(-\frac{T_2}{m_2}+n+\frac{T_1}{m_2}-a+\frac{2aS^*}{k})\lambda+\frac{nT_1}{m_2}\\ +\frac{aT_2}{m_2}-\frac{2aT_2S^*}{m_2k}-a+\frac{2aS^*}{k}=0. \end{aligned} \tag{3.12}$$

If the characteristic equation satisfies the following conditions

$$-\frac{T_2}{m_2}+n+\frac{T_1}{m_2}-a+\frac{2aS^*}{k}>0,$$

$$\frac{nT_1}{m_2}+\frac{aT_2}{m_2}-\frac{2aT_2S^*}{m_2k}-a+\frac{2aS^*}{k}>0,$$

$$(-\frac{T_2}{m_2}+n+\frac{T_1}{m_2}-a+\frac{2aS^*}{k})^2-4(\frac{nT_1}{m_2}+\frac{aT_2}{m_2}-\frac{2aT_2S^*}{m_2k}-a+\frac{2aS^*}{k})>0.$$

it can be obtained that the characteristic equation has two negative roots in the region A_2, which means that the point $\tilde{E}_2$ is locally asymptotically stable. □

4. Optimal control strategies

In this section, we investigate the dynamic behaviors of the system under control variables $u_1(t)$ and $u_2(t)$. The first control equation $u_1(t)$ is to enhance prevention strategies, reduce the number of patients, vaccinate and wear masks, or increase social distance. This control can reduce the probability of illness among susceptible populations, represented by $(1-u_1(t))$. The second control equation $u_2(t)$ represents accelerating the recovery time of patients, enhancing medical conditions, developing specific drugs, and enhancing human immune capacity. We focus on the impact of media factor m_1 on the infected individuals, while ignoring the impact of m_2 on infection rates. We set $m_1 \neq 0, m_2 = 0$ and the system becomes

$$\begin{cases} \dfrac{\mathrm{d}S}{\mathrm{d}t} = aS(1-\dfrac{S}{k}) - e^{-m_1 I}bIS(1-u_1(t)), \\ \dfrac{\mathrm{d}I}{\mathrm{d}t} = e^{-m_1 I}bIS(1-u_1(t)) - \alpha I - \beta I - (\gamma + u_2(t))I, \\ \dfrac{\mathrm{d}R}{\mathrm{d}t} = (\gamma + u_2(t))I - \mu R. \end{cases} \tag{4.1}$$

When $u_i = 1, (i = 1, 2)$ indicates complete control, and $u_i = 0$ indicates that control is ineffective, we consider the following optimal control problem to minimize the objective functional as given by

$$J(u_1, u_2) = \min_{0\le u_1, u_2 \le 1} \int_0^{T_f} (\omega_1 I + \frac{1}{2}[\omega_2 u_1^2(t) + \omega_3 u_2^2(t)])dt. \tag{4.2}$$

The weight constant ω_1 represents the infected population, while ω_2 and ω_3 represent the weight constants of personal protection and improvement of medical conditions, respectively. The terms $\frac{1}{2}\omega_2 u_1^2(t)$ and $\frac{1}{2}\omega_3 u_2^2(t)$ describe the costs associated with the corresponding intervention measures over the time interval $[0, T_f]$. Assuming that the cost is proportional to the square of the corresponding control function, we have

$$J(u_1^*, u_2^*) = \min\{J(u_1, u_2) : u_1, u_2 \in \mathcal{U}\}$$

where $\mathcal{U}$ is defined by

$$\mathcal{U} = \{(u_1, u_2) \mid 0 \le u_1, u_2 \le 1\}$$

for $t \in [0, T_f]$. Therefore, in order to determine the necessary conditions that the optimal control (u_1^*, u_2^*) must satisfy, Pontryagin's maximum principle is used [29] and the Hamiltonian $\mathcal{H}$ for the control problem is defined by:

$$\begin{aligned}\mathcal{H} =&\omega_1 I + \frac{1}{2}[\omega_2 u_1^2(t) + \omega_3 u_2^2(t)] \\ &+ \lambda_1[aS(1 - \frac{S}{k}) - e^{-m_1 I} bIS(1 - u_1(t))], \\ &+ \lambda_2[e^{-m_1 I} bIS(1 - u_1(t)) - \alpha I - \beta I - (\gamma + u_2(t))I], \\ &+ \lambda_3[(\gamma + u_2(t))I - \mu R]\end{aligned} \tag{4.3}$$

and the adjoint variables $\lambda_i (i = 1, 2, 3)$ are associated with the state variables of the model (4.1). The expression satisfies the following:

$$\begin{aligned}\frac{\mathrm{d}\lambda_1}{\mathrm{d}t} &= e^{-m_1 I} bI(1 - u_1(t))(\lambda_1 - \lambda_2) - a\lambda_1 + 2\lambda_1 S\frac{a}{k}, \\ \frac{\mathrm{d}\lambda_2}{\mathrm{d}t} &= (-m_1 e^{-m_1 I} bIS + e^{-m_1 I} bS)(1 - u_1(t))(\lambda_1 - \lambda_2) \\ &\quad + (\alpha + \beta)\lambda_2 - (\gamma + u_2)\lambda_3 + \gamma + u_2(t) - \omega_1, \\ \frac{\mathrm{d}\lambda_3}{\mathrm{d}t} &= \mu\lambda_3\end{aligned} \tag{4.4}$$

with the terminal (transversality) conditions $\lambda_i(T_f) = 0, i = 1, 2, 3$. Further, the optimal control double (u_1^*, u_2^*) is given as follows:

$$\begin{aligned}u_1^* &= \max\{0, \min\{1, \frac{e^{-m_1 I} bIS(\lambda_2 - \lambda_2)}{\omega_2}\}\}, \\ u_2^* &= \max\{0, \min\{1, \frac{I(\lambda_2 - \lambda_2)}{\omega_3}\}\}.\end{aligned} \tag{4.5}$$

5. Numerical simulations

In this section, we use numerical simulations to verify the rationality of the theory. Figures 1 and 2 display the relationship between the dynamic of the system and R_0. When $R_0 < 1$, the disease-free equilibrium point $(k, 0)$ of the system is located in region A_1 or A_2, depending on the values of m_1 and m_2. Figure 1(a) displays the equilibrium point as located in A_1. It can be observed that changing different initial values of the system will cross the line $S = S_q$ and stabilize at the equilibrium point. The equilibrium point is located at A_2 in Figure 1(b). It can be found that the trajectory starting from A_2 will stabilize at the equilibrium point, while the trajectory with an initial value at A_1 will directly pass through $S = S_q$ to reach the equilibrium point at A_2. On the other hand, when $R_0 > 1$, the system dynamics are displayed in Figure 2. Any trajectory with an initial value at A_1 or A_2 will directly pass through $S = S_q$ to stabilize at point $\tilde{E}_2$, which is regular and is globally asymptotically stable in A_2.

The system is not influenced by media factors, as described in Figure 3(a). When $R_0 > 1$, the number of diseases $I(t)$ asymptotically stabilizes at a steady-state value. When $R_0 < 1$, $I(t)$ exhibits a downward trend and achieves the desired control effect. In Figure 3(b), the media factor parameters are $m_1 = 0.2$, $m_2 = 0.8$. The situation is similar to Figure 3(a), but when $R_0 < 1$, the media related parameters m_1 and

m_2 have no effect on the number of diseases. This indicates that when the basic reproduction number is $R_0 < 1$, the influence of media factors on the system is not significant. In a word, when infectious diseases spread, media factors should be utilized at appropriate times to influence the disease.

The values of media-related parameters m_1 or m_2 are changed to explore the influence of media factors on diseases. In Figure 3(c), the peak value of $I(t)$ has a slight backward movement at the increase of the m_2 value. Figure 3(d) indicates that the peak value decreases with the increase of m_1 and the peak appearance time is slightly earlier. It is interesting to note that media reports need to choose certain methods to ensure a positive impact on disease control. This depends on the authenticity of media reports and the popularity of media reporting platforms.

The effects of parameters m_1 and m_2 on the infected population is shown in Figure 4, where the color bar represents the fluctuation height. Without the influence of parameter m_1, the system fluctuation moves backward with the increase of m_2, and the phenomenon of backward fluctuation is significant at the m_2 close to 1. When m_1 is magnified to 0.2, the fluctuation moves backward slowly. Interestingly, the situation of $m_2 = 0$ is different from $m_1 = 0$. As m_1 increases, the second wave of $I(t)$ shifts significantly forward. If $m_2 = 0.4$, the system fluctuations and changes are not significant.

Sensitivity analysis can analyze and understand the impact of different parameters on specific variables, which may help us control disease transmission or provide guidance. Referring to the definition in [27], the sensitivity index of R_0 for each parameter c is defined as follows:

$$\mathcal{L}_c^{R_0} = \frac{\partial R_0}{\partial c} \times \frac{c}{R_0}.$$

Among all positive correlation factors in Fig.5, the population carrying capacity k and basic transmission coefficient b are the highest. This indicates that the value of k or b is positively correlated to R_0 with a degree of 100%. However, among all the negative correlation factors, the rate of recovery from infection γ is the most sensitive parameter, and the value of γ is negatively correlated to R_0 with a degree of 78.95%.

The numerical simulation of the optimal control system is implemented using MATLAB, and the equation is solved using the forward backward of the fourth order Runge-Kutta method [28]. The weight constants are chosen as $\omega_1 = 50, \omega_2 = 100$, and $\omega_3 = 1$. Figure 6(a) exhibits the time history of two controls u_1 and u_2 coexisting and Figure 6(d) represents the disease population quickly reaching the minimum value under dual-control. Figure 6(b,c) investigates the dynamics of the system under a single control of u_1 and u_2, corresponding to Figure 6(e,f). It is worth noting that under a single control, u_1 has a stronger control effect on the disease population, while u_2 can reduce the peak of the disease population.

From the perspective of epidemics, maintaining an effective social distance under the influence of control u_1 reduces the probability of illness in susceptible populations and achieves the effect of controlling the total number of infectious diseases as quickly as possible in a limited period of time. Under the influence of control u_2, the effect of controlling the number of diseases is achieved relatively slowly in a short period of time by accelerating the recovery time of patients and improving medical conditions. Under the influence of both control strategies, the effect of controlling the number of diseases is stronger and faster, which provides ideas for the prevention of epidemics.

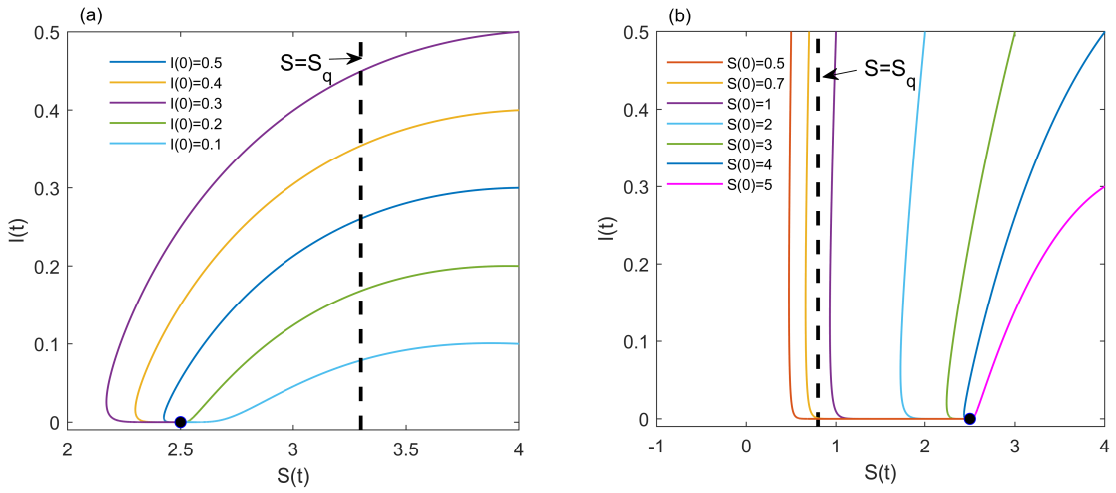

Figure 1. The phase diagram of the SIR model under the case of $R_0 = 0.6579 < 1$. The dotted line indicates $S = S_q$, the left side of the dotted line is the A_1 area, and the right side is the A_2 area. The black point is the equilibrium point of disease elimination E_0^* and the parameters are $b = 0.5, r = 1.5, \beta = 0.2, \alpha = 0.2, k = 2.5, a = 0.1, \mu = 0.1$ (a) $S(0) = 4, m_1 = 0.2, m_2 = 0.8$; (b) $I(0) = 0.5, m_1 = 0.6, m_2 = 0.4$.

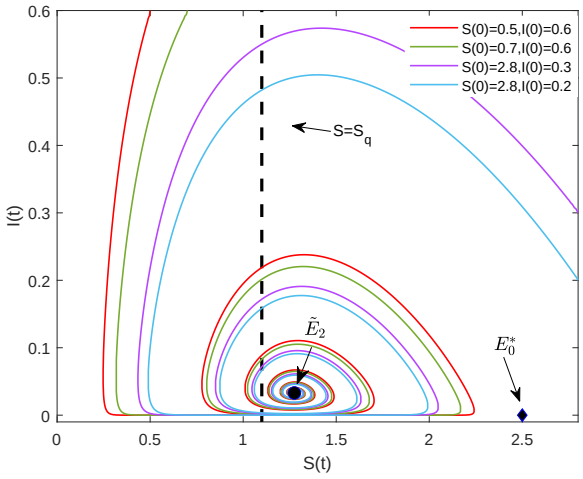

Figure 2. The phase diagram of the SIR model under the case of $R_0 = 1.9737 > 1$. The dotted line indicates $S = S_q$, the left side of the dotted line is the A_1 area, and the right side is the A_2 area. The black points are the local equilibrium points E_0^* and $\tilde{E}_2$ and the parameters are $b = 1.5, r = 1.5, \beta = 0.2, \alpha = 0.2, k = 2.5, a = 0.1, \mu = 0.1, m_1 = 0.2, m_2 = 0.8$.

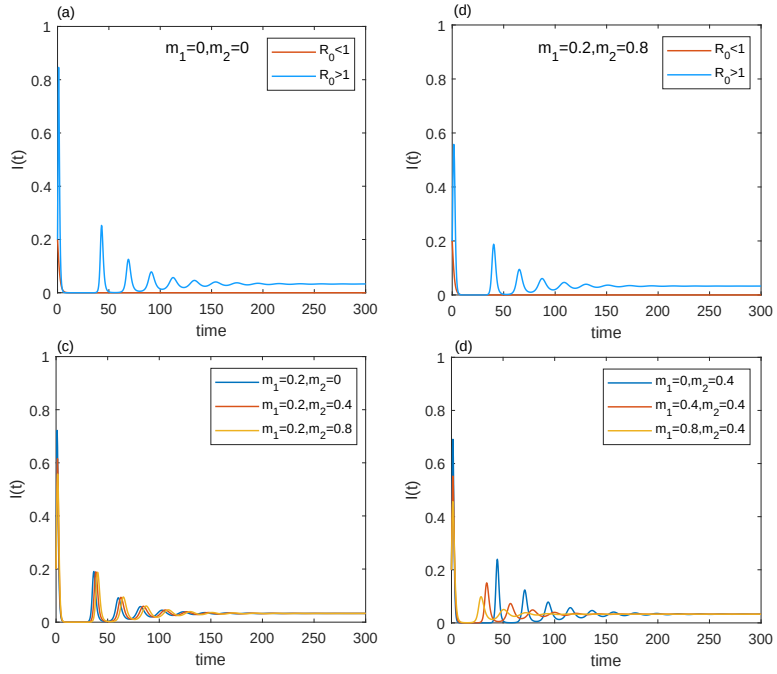

Figure 3. The time history diagram of disease I(t) and the model select different parameters under the case of $R_0 < 1$ (red line) and $R_0 > 1$ (blue line),(a) m_1=0, m_2=0; (b) m_1=0.2, m_2=0.8; (c) In the case of $m_1 = 0.2$, $m_2 = 0$, 0.4 or 0.8. (d) $m_2 = 0.4$, $m_1 = 0$, 0.4 or 0.8.

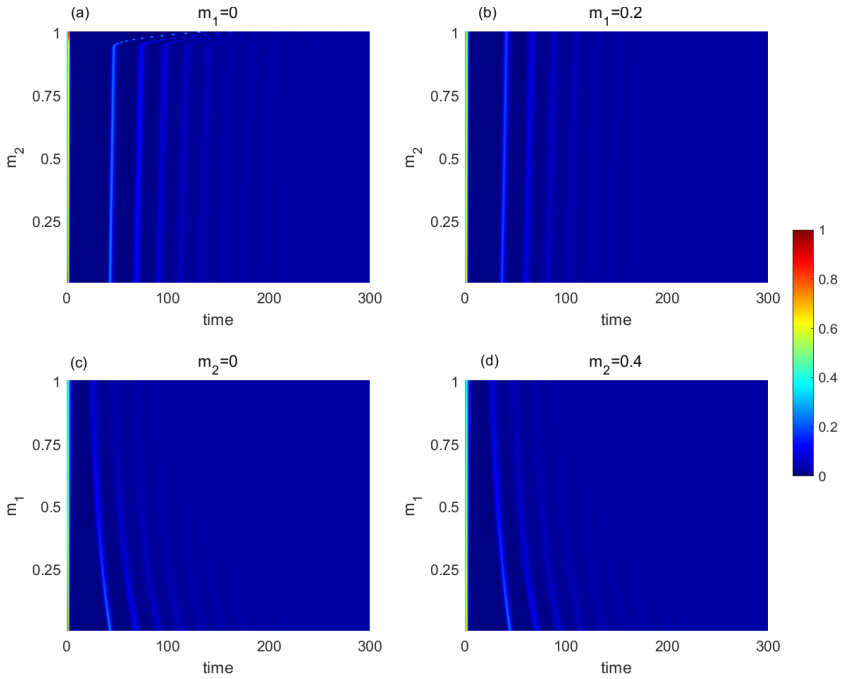

Figure 4. The influence of parameters m_1 and m_2 on $I(t)$. (a) The system fix $m_1 = 0$ and (b) $m_1 = 0.2$, (c) fix $m_2 = 0$ and (d) $m_1 = 0.4$.

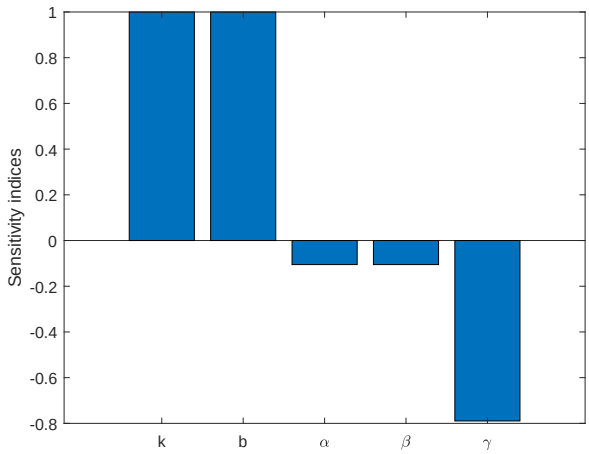

Figure 5. The model sensitivities to its associate parameters.

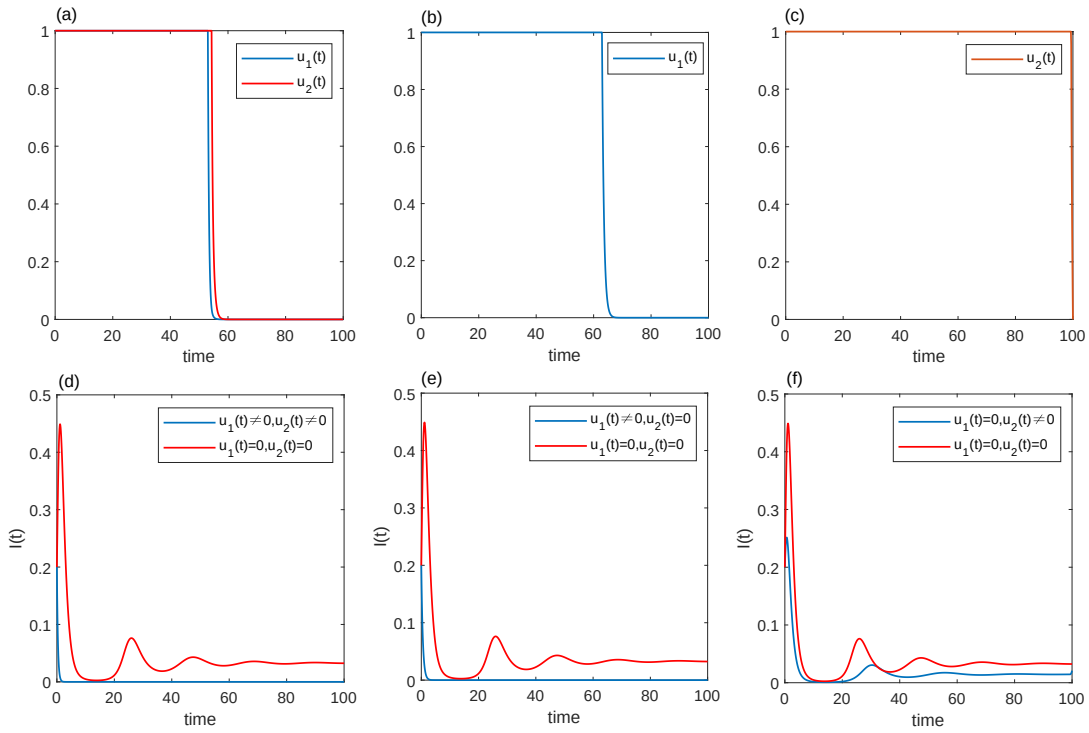

Figure 6. (a) Combined effects of optimal controls $u_1(t)$, $u_2(t)$ on the system. (b) or (c) Control profile ($u_1(t)$ or $u_2(t)$) and its effects on the system. (d–f) Time history diagrams under different control situations of $I(t)$.

6. Conclusions

Inspired by COVID-19, this paper constructed an epidemic model to include media factors to explore the control effects of media factors on diseases. In the theoretical analysis, the media factor uses the Lambert W function to transform the system defined by the implicit function into the displayed PWS function. The research results indicated that the media factor has an obvious control effect on the epidemic situation under the basic reproduction number $R_0 > 1$, which verifies that the media has an inhibitory effect on disease.

Sensitivity analysis, as a method of analyzing parameters, revealed that the population carrying capacity k and basic transmission coefficient b are positively correlated with R_0, while the rate of recovery from infection γ is negatively correlated with R_0. This may provide a control strategy for disease control. Finally, the optimal control strategy was designed to analyze the impact of different controls on the system. It can be concluded that dual-control has the best effect on disease control. This result may provide methods for epidemic control.

Use of AI tools declaration

The authors declare they have not used Artificial Intelligence (AI) tools in the creation of this article.

Acknowledgments

This work was supported by a grant from the Natural Science Foundation of Inner Mongolia (Grants No. 2022MS01011).

Conflict of interest

The authors have no conflicts of interest to declare.

References

1. R. Wijk, L. Mockeliunas, G. Hoogen, C. Upton, A. Diacon, U. Simonsson, Reproducibility in pharmacometrics applied in a phase III trial of BCG-vaccination for COVID-19, *Sci. Rep.*, **13** (2023), 16292. https://doi.org/10.1038/s41598-023-43412-3
2. Y. Bai, L. Yao, T. Wei, F. Tian, D. Y. Jin, L. Chen, et al., Presumed asymptomatic carrier transmission of COVID-19, *JAMA*, **323** (2020), 1406–1407. https://doi.org/10.1001/jama.2020.2565
3. *WHO COVID-19 dashboard*, World Health Organization, 2023. Available form: `https://covid19.who.int`.
4. S. Olaniy, O. S. Obabiyi, K. O. Okosun, A. T. Oladipo, S. O. Adewale, Mathematical modelling and optimal cost-effective control of COVID-19 transmission dynamics, *Eur. Phys. J. Plus*, **135** (2020), 938. https://doi.org/10.1140/epjp/s13360-020-00954-z

5. B. Salzberger, T. Gl*ü*ck, B. Ehrenstein, Successful containment of COVID-19: the WHO-Report on the COVID-19 outbreak in China, *Infection*, **48** (2020), 151–153. https://doi.org/10.1007/s15010-020-01409-4

6. S. Goel, S. Bhatia, J. Tripathi, S. Bugalia, M. Rana, V. Bajiya, SIRC epidemic model with cross-immunity and multiple time delays, *J. Math. Biol.*, **87** (2023), 42. https://doi.org/10.1007/s00285-023-01974-w

7. X. Huo, J. Chen, S. Ruan, Estimating asymptomatic, undetected and total cases for the COVID-19 outbreak in Wuhan: a mathematical modeling study, *BMC Infect. Dis.*, **21** (2021), 476. https://doi.org/10.1186/s12879-021-06078-8

8. S. Bergeron, A. Sanchez, Media effects on students during SARS outbreak, *Emerging Infect. Dis.*, **11** (2005), 732. https://doi.org/10.3201/eid1105.040512

9. J. Cui, Y. Sun, H. Zhu, The impact of media on the control of infectious diseases, *J. Dyn. Diff. Equat.*, **20** (2008), 31–53. https://doi.org/10.1007/s10884-007-9075-0

10. K. Louis, M. F. Shannon, M. Natasha, S. Jeffrey, Incorporating media data into a model of infectious disease transmission, *PLoS ONE*, **14** (2019), e0197646. https://doi.org/10.1371/journal.pone.0197646

11. R. J. Blendon, J. M. Benson, C. M. Desroches, E. Raleigh, K. Taylor-Clark, The public's response to severe acute respiratory syndrome in Toronto and the United States, *Clin. Infect. Dis.*, **38** (2004), 925–931. https://doi.org/10.1086/382355

12. Y. Xiao, T. Zhao, S. Tang, Dynamics of an infectious disease with media/psychology induced non-smooth incidence, *Math. Biosci. Eng.*, **10** (2013), 445–461. https://doi.org/10.3934/mbe.2013.10.445

13. C. Sun, W. Yang, J. Arino, K. Khan, Effect of media-induced social distancing on disease transmission in a two patch setting, *Math. Biosci.*, **230** (2011), 87–95. https://doi.org/10.1016/j.mbs.2011.01.005

14. S. L. Bergeron, A. L. Sanchez, Media effects on students during SARS outbreak, *Emerg. Infect Dis.*, **11** (2005), 732–734. https://doi.org/10.3201/eid1105.040512

15. I. Dhaoui, W. V. Bortel, E. Arsevska, C. Hautefeuille, S. T. Alonso, E. V. Kleef, Mathematical modelling of COVID-19: a systematic review and quality assessment in the early epidemic response phase, *Int. J. Infect. Dis.*, **116** (2022), S110. https://doi.org/10.1016/j.ijid.2021.12.260

16. R. K. Rai, A. K. Misra, Y. Takeuchi, Modeling the impact of sanitation and awareness on the spread of infectious diseases, *Math. Biosci. Eng.*, **16** (2019), 667–700. https://doi.org/10.3934/mbe.2019032

17. Y. Yang, L. Zou, J. Zhou, S. Ruan, Dynamics of a nonlocal viral infection model with spatial heterogeneity and general incidence, *J. Evol. Equ.*, **23** (2023), 29. https://doi.org/10.1007/s00028-023-00879-x

18. D. Kalajdzievska, M. Li, Modeling the effects of carriers on transmission dynamics of infectious diseases, *Math. Biosci. Eng.*, **8** (2011), 711–722. https://doi.org/10.3934/mbe.2011.8.711

19. B. Pell, S. Brozak, T. Phan, F. Wu, Y. Kuang, The emergence of a virus variant: dynamics of a competition model with cross-immunity time-delay validated by wastewater surveillance data for COVID-19, *J. Math. Biol.*, **86** (2023), 63. https://doi.org/10.1007/s00285-023-01900-0

20. J. Jia, J. Ding, S. Liu, G. Liao, J. Li, B. Duan, et al., Modeling the control of COVID-19: impact of policy interventions and meteorological factors, *arXiv*, 2020. https://doi.org/10.48550/arXiv.2003.02985

21. H. Huang, Y. Chen, Z. Yan, Impacts of social distancing on the spread of infectious diseases with asymptomatic infection: a mathematical model, *Appl. Math. Comput.*, **398** (2021), 125983. https://doi.org/10.1016/j.amc.2021.125983

22. C. Maji, F. Al-Basir, D. Mukherjee, K. S. Nisar, C. Ravichandran, COVID-19 propagation and the usefulness of awareness-based control measures: a mathematical model with delay, *AIMS Math.*, **7** (2022), 12091–12105. https://doi.org/10.3934/math.2022672

23. O. Diekmann, J. A. P. Heesterbeek, *Mathematical epidemiology of infectious diseases: model building, analysis and interpretation*, John Wiley & Son, Ltd., 2000.

24. H. W. Hethcote, The mathematics of infectious diseases, *SIAM Rev.*, **42** (2000), 599–653. https://doi.org/10.1137/S0036144500371907

25. R. Corless, G. Gonnet, D. Hare, D. Jeffrey, D. Knuth, On the Lambert W function, *Adv. Comput. Math.*, **5** (1996), 329–359. https://doi.org/10.1007/BF02124750

26. M. D. Bernardo, C. J. Budd, A. R. Champneys, P. Kowalczyk, A. B. Nordmark, G. O. Tost, et al., Bifurcations in nonsmooth dynamical systems, *SIAM Rev.*, **50** (2008), 629–701. https://doi.org/10.1137/050625060

27. H. Nasir, A time-delay model of diabetic population: dynamics analysis, sensitivity, and optimal control, *Phys. Scr.*, **96** (2021), 115002. https://doi.org/10.1088/1402-4896/ac1473

28. S. Lenhart, J. T. Workman, *Optimal control applied to biological models*, New York: Chapman and Hall/CRC, 2007. https://doi.org/10.1201/9781420011418

29. L. S. Pontryagin, V. G. Boltyanskii, R. V. Gamkrelidze, E. F. Mishchenko, *The mathematical theory of optimal processes*, New York: John Wiley and Sons, Inc., 1962.

AIMS Press